Journal of The Electrochemical Society, **152** (12) H213-H218 (2005)
0013-4651/2005/152(12)/H213/6/$7.00 © The Electrochemical Society, Inc.

Combinatorial Screening and QSAR Modeling in the $SrO–B_2O_3–P_2O_5$ Ternary System to Search for Thermally Stable Blue Phosphors for PDPs

Kee-Sun Sohn,[a,z] Jeong Gon Yoo,[a] Namsoo Shin,[b] Kenji Toda,[c] and Dong-Sik Zang[d]

[a]*Department of Materials Science and Metallurgical Engineering, Sunchon National University, Suncheon, Chonnam 540-742, Korea*
[b]*Pohang Accelerator Laboratory, Beamline Division, Pohang, Kyungbuk 790-784, Korea*
[c]*Graduate School of Science and Technology, Niigata University, Niigata City 950-2181, Japan*
[d]*Samsung SDI Company, Limited, Corporate Research and Development Center, Kyeonggi 449-902, Korea*

The need to identify a thermally stable blue phosphor for plasma display panels (PDPs) is vital, because the currently used $BaMgAl_{10}O_{17}:Eu^{2+}$ (BAM) phosphors have serious thermal degradation problems. In this respect, we report on the screening of a Eu^{2+}-doped $SrO–B_2O_3–P_2O_5$ system by a combinatorial chemistry technique so that combinatorial libraries could be developed in terms of luminance and color chromaticity. As a quantitative structure activity relationship (QSAR) model, a continuous luminance map was obtained as a function of composition using an artificial neural network trained using the results from the combinatorial screening. Promising photoluminescence was found in a lineshape composition range in the $SrO–B_2O_3–P_2O_5$ ternary library, and the samples in this composition range were crystallized into a single major phase of $Sr_6BP_5O_{20}:Eu^{2+}$ in an $I\bar{4}c2$ symmetry with cell parameters $a = 9.784$ and $c = 19.01$. The luminance of $Sr_6BP_5O_{20}:Eu^{2+}$ was 2.8 times as high as BAM under vacuum ultraviolet (VUV) excitation and underwent negligible thermal degradation, even though the CIE color chromaticity was somewhat poor.
 [DOI: 10.1149/1.2083208]

Manuscript submitted May 6, 2005; revised manuscript received July 1, 2005. Available electronically October 17, 2005.

$BaMgAl_{10}O_{17}:Eu^{2+}$ (BAM) phosphors are typically used as a blue component in plasma display panels (PDPs).[1-6] However, the degradation of its luminescent intensity either in preparation or in use is one of the most significant shortcomings of the application. The origin of the degradation is thermal heating at temperatures up to 450°C during the sealing process and erosion by plasma or vacuum ultraviolet (VUV) photons during use. In an attempt to overcome this obstacle, considerable efforts have been made in two areas. First, the exact degradation mechanism of BAM has been studied by examining both the structural and luminescent properties in order to improve BAM phosphors.[2-6] More importantly, other research groups have attempted to find new substitutes for BAM phosphors, and, as a result, several tentative solutions have been obtained.[7-9] It is unfortunate, however, that none of these solutions are sufficiently satisfactory to completely rule out the thermal degradation problem. For example, even though two alternatives such as $Sr_3Al_{10}SiO_{20}:Eu^{2+}$ (SAS)[7] and $CaMgSi_2O_6:Eu^{2+}$ (CMS)[9] have recently been developed, the former still has a thermal degradation problem, and the luminescent efficiency of the latter is too low under VUV excitation. Accordingly, neither SAS nor CMS can be substituted for BAM at this time. A new blue phosphor that surpasses BAM in terms of luminescent efficiency under VUV excitation and which is thermally stable is needed.

We screened a Eu^{2+}-doped $SrO–B_2O_3–P_2O_5$ system by means of a combinatorial chemistry technique to search for new blue phosphors for use in PDP applications. Our combinatorial chemistry system, which is based on solution pyrolysis, includes high throughput synthesis and characterization, details of which were described in our previous reports.[10-14] A $SrO–B_2O_3–P_2O_5$ ternary combinatorial library was prepared in advance and more accurate libraries were subsequently prepared in sequence based on the results of former screenings. Such a serial library technique, so-called fine-tuning or zoom-up, has proven to be an efficient strategy for the development of new material in a given composition system, e.g., a ternary or quaternary system.[11,13] Based on our ternary combinatorial libraries, quantitative structure activity relationships (QSARs) were obtained using an artificial neural network (ANN). That is, the luminescent intensity and CIE chromaticity were expressed as a function of composition over a limited range. The combinatorial screening made it possible to find a promising stoichiometry range in view of luminescent efficiency at VUV excitation

Experimental

Eu^{2+}-doped $SrO–B_2O_3–P_2O_5$ ternary combinatorial libraries were produced by a solution-based synthesis method based on the combinatorial screening technique. The amount of Eu^{2+} doping was fixed at a value (1/100 of SrO in mol %) for all the libraries. All the law powders [except for europium oxide (Eu_2O_3)], such as strontium nitrate [$Sr(NO_3)_2$], boric acid (HBO_3), and diammonium hydrogen phosphate [$(NH_4)_2HPO_4$], were dissolved in deionized water and the Eu_2O_3 was dissolved in dilute nitric acid. The correct amount of each solution was then injected into each sample site in a specially designed quartz glass container (given the name "combi-chem" container) according to the composition table. The solutions in the combi-chem container were dried at 100°C for 48 h and further dried at 600°C for 6 h. The dried samples were pulverized and successively fired at 1200°C in a reducing atmosphere. The reducing atmosphere was produced by introducing a mixture of nitrogen and a certain amount of hydrogen (25%) into the furnace so that the desired oxidation state of the activator ions (Eu^{2+}) could be achieved.

Some of the samples chosen among the library were removed from the combi-chem containers and examined by synchrotron radiation X-ray diffraction (SR-XRD). SR-XRD measurements of selected samples were performed in the 8C2 high-resolution powder diffraction (HRPD) beamline at the Pohang Accelerator Laboratory. The emission spectra used for the combinatorial libraries were monitored at 254 nm with the samples being left in the combi-chem containers using a plate reader accessory attached to a Perkin Elmer LS50B spectrometer with a xenon flash lamp. Eight representative samples were taken from the combi-chem containers and the emission spectra were measured at 147 nm excitation using a Kr_2 lamp in a vacuum chamber. Even though 147 nm excitation was not employed for all the samples, it was verified that the results at 254 nm excitation were in good agreement with those at 147 nm by an auxiliary, confirmatory experiment in which the results at 254 and 147 nm were compared for several selected samples. The emission and excitation spectra in the VUV and UV range were measured using a photoluminescence (PL) system, which included a D2 lamp, vacuum chamber, vacuum monochromator for excitation light

[z] E-mail: kssohn@sunchon.ac.kr

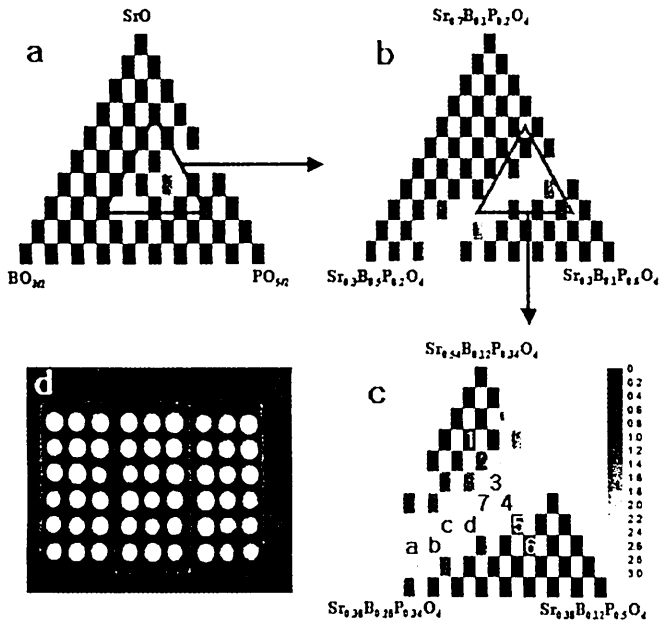

Figure 1. Ternary combinatorial libraries of (a) first screening, (b) second fine-tuning, and (c) third fine-tuning in terms of luminance at an excitation light wavelength of 147 nm, and (d) the actual library photographed under 254-nm excitation.

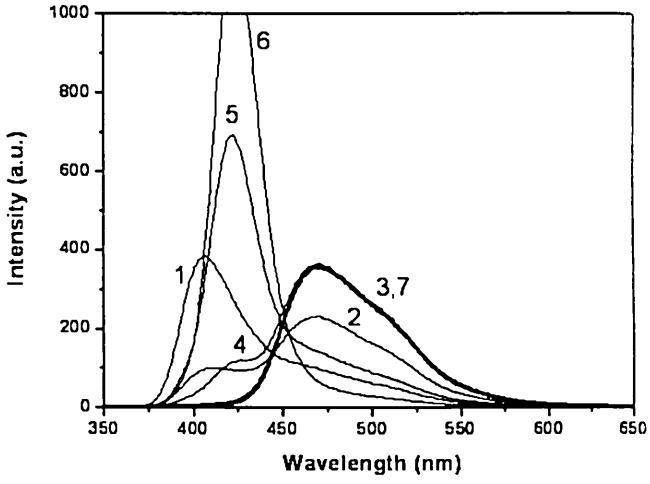

Figure 2. Emission spectra of numbered samples removed from the final screening library.

monochrotizing, emission monochromator, photomultiplier tubes, and a controlling unit. The excitation spectra were measured in the range from 140 to 300 nm using sodium salicylate powder as a reference. Luminance was calculated by integrating the product of the emission spectrum and the standard visual spectral efficiency curve based on the CIE regulation.[15] Time-resolved emission spectra were also obtained using a femto second Nd: yttria aluminum garnet (YAG) laser and a charge coupled device (CCD) sensor with a 20 ns time resolution, and photoluminescent decay curves were obtained from the time-resolved spectra. The excitation wavelength was 355 nm, produced by tripling the 1066-nm frequency of the Nd:YAG laser.

Results and Discussion

Combinatorial Screening.— Figure 1 shows the Eu^{2+}-doped $SrO–B_2O_3–P_2O_5$ ternary combinatorial libraries in terms of luminance at an excitation wavelength of 254 nm. The indication of composition in these libraries does not designate real values of synthesized samples but applied values that were determined prior to synthesis. The discussion regarding the exact composition of the synthesized samples and the method used for determining the exact composition are addressed below. Figure 1a shows the first screened library, and the ensuing fine-tunings are represented in Fig. 1b and Fig. 1c. In all the libraries, the brighter the rectangular spot, the higher the luminance. The numbers adjacent to the scale bar represent luminance values relative to that of BAM. A promising region of high luminance began to be conspicuous in the first fine-tuning, as shown in Fig. 1b. It is clear that a slant line-shaped bright region was formed in the library from the first fine-tuning, as can be seen in Fig. 1b. Thus, we chose a more restricted area for another fine-tuning, as indicated by a small triangle in Fig. 1b, thereby providing the final library shown in Fig. 1c. A line-shaped high-luminance region spanning from the upper right to the lower left was also conspicuous in the final fine-tuning library. Figure 1d shows an actual library photographed at an excitation light wavelength of 254 nm.

Figure 2 shows emission spectra of several representative samples, the composition of which are located on the line crossing the high-luminance region in the final library. All of the spectra in Fig. 2 are numbered so that they can be identified in the final library, as can be seen in Fig. 1c. Some samples, which are located on the boundary area of the line-shaped high-luminance region, show secondary peaks in the PL spectrum. These peaks at around 407 and 422 nm appear to originate from undesirable, minor phosphate phases such as $Sr_3(PO_4)_2$ and $Sr_2P_2O_7$, respectively.[16] Such a finding was also verified by our structural analysis, which is discussed in the section on $Sr_6BP_5O_{20}:Eu^{2+}$ blue phosphor. Both $Sr_3(PO_4)_2:Eu^{2+}$ and $Sr_2P_2O_7:Eu^{2+}$ are well-known, commercially available blue phosphors used for photocopy machines but they are not practically useful from the point of view of its use in PDP applications. The evolution of the shape of the emission spectra with respect to composition was monitored proceeding from sample 1 to 6. It is noteworthy that the emission spectrum of samples located in the high-luminance region did not exhibit such secondary peaks. When proceeding further from the high-luminance region, the secondary peak became stronger and eventually only the secondary peak remains in a sufficiently remote area from the high-luminance region, similar to samples 1, 5, and 6. In addition, it is also obvious that the samples in the area above the high-luminance area showed a 407-nm peak, whereas the area beneath the high-luminance area showed a 422-nm peak. We did not investigate these undesirable peaks in more detail in the present investigation, because their presence was indicative of the fact that these compositions were not well crystallized into a single-phase compound. Samples exhibiting only a main emission peak at 470 nm without any secondary peaks were of major concern and are marked with open circles. Those exhibiting undesirable, secondary peaks at around 407 and 422 nm are marked with solid circles in the final library, as can be seen in Fig. 3c.

Acceptable luminance was obtained in the composition range of $0.41 < Sr < 0.48$, $0.12 < B < 0.23$, and $0.39 < P < 0.42$, as can be seen in the library for the last fine-tuning. The slant line-shaped high-luminance region was located in such a direction in which the amount of boron varies considerably. This indicates that boron did not have a significant influence on luminance in the range from 0.12 to 0.23. More importantly, the Sr/P atomic ratio varied between 1.1 and 1.2 and the Sr/B ratio was in the range from 1.7 to 4. The luminance values in the high-luminance region were much higher than that of BAM, by 250–280%. The phase identification revealed that all the compositions in this high-luminance region were apt to crystallize into a single phase and to contain a negligible amount of minor phases. The phase identification and structural analysis is discussed in more detail later.

The CIE color chromaticity was also represented in the ternary library as can be seen in Fig. 3a-c. The brightness of each rectangular spot of libraries in Fig. 3a-c is indicative of y values for the CIE

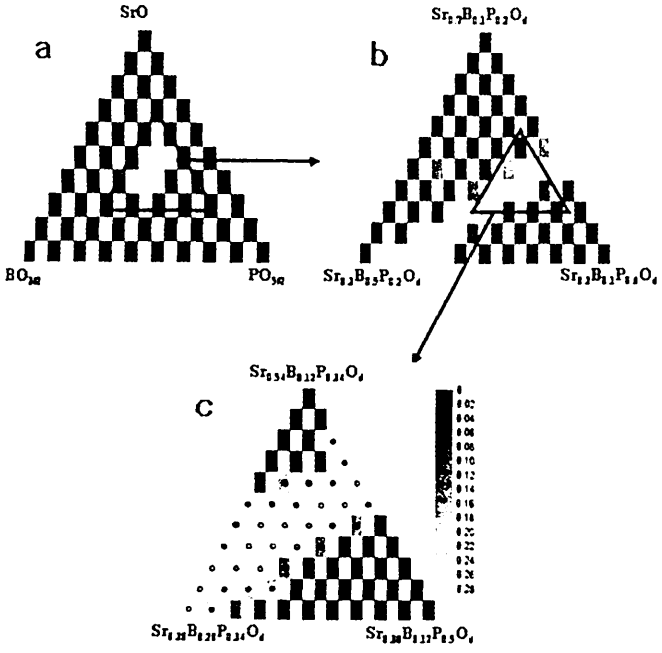

Figure 3. Ternary combinatorial libraries of (a) first screening, (b) second fine-tuning, and (c) third fine-tuning in terms of the CIE chromaticity coordinate y at the excitation light wavelength of 147 nm.

chromaticity coordinates, similar to the luminance libraries in Fig. 1a-c. It is customary to consider the y value only in the case where bluish colors are concerned, because the x value remains within a very narrow range around the standard value and, in fact, did not vary significantly in our case. The y values in the high-luminance region were in the range from 0.25 to 0.28. These values are deviated from the value ($y = 0.08$) of the standard blue color declared by the National Television Standard Committee (NTSC). The y value should be improved considerably, to a value closer to the standard blue color. This deviation would be reduced by employing the secondary peaks at 407 and 422 nm that play a positive role in reducing the y value. In particular, the 422 nm peak could be of practical use if it were balanced with the main peak at 470 nm. Thus, regarding only the CIE color chromaticity, rather than the luminance, the edge area around the slant line-shaped high-luminance region would be more advantageous. As mentioned above, however, this edge area was not crystallized into a single major phase, and as a result, the chemical stability would be expected to be poor. More seriously, the luminance would be dramatically decreased, considering the fact that the standard visual spectral efficiency curve has a value of nearly zero at wavelengths below 420 nm. A tangible method for improving color chromaticity without a serious drop in luminance is presented later.

QSAR.— If luminance could be expressed as a definite function of composition, it could be an ideal completion of the combinatorial screening process. Unfortunately, however, it is theoretically impossible to find such types of analytical nonlinear functions. In contrast to a theoretical approach, it is possible to obtain a stochastic relationship between luminance and composition. In this regard, some efforts have been made to develop methodologies for acquiring QSAR models. The most popular method for obtaining QSAR models is the use of trained artificial neural networks (TANN).[17-21] It is well known that TANN permits unknown (or unmeasured) data to be predicted by intra- and extrapolating experimental data appropriately, although it cannot provide a definite analytical function form. TANN is a good approximation for QSAR, so that a trend in some data can be easily understood in a systematic manner. However, TANN is versatile only for QSAR modeling. It would be useless if

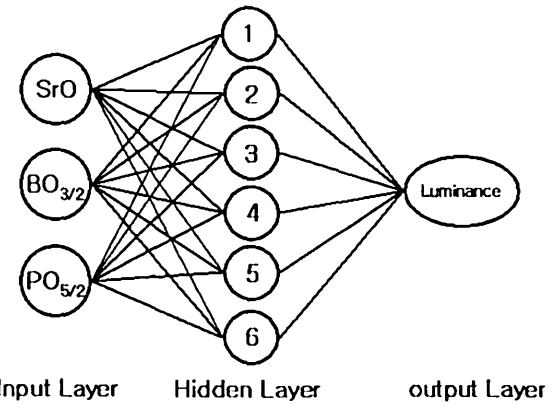

Figure 4. Architecture of the three-layered artificial neural network.

one were to predict a much higher activity (luminance in this case) than the actually measured data used for the training set by adopting global or local optimization strategies. Even though several research groups have used TANNs to optimize heterogeneous catalytic materials[17-19] or to hybridize it with other global optimization strategies such as a genetic algorithm,[20,21] it is our opinion that the optimization of TANN can never yield a much higher activity than the initial data used for the training. In this regard, TANN can never be utilized for the prediction of the optimum composition of a compound, the luminance of which is substantially higher than the highest member in the initial training data. This could be easily understood by considering the nature of artificial neural networks.[22] That is, the optimization result is wholly dependent on the initial data set used for the training. It is certain that the optimum composition would be determined around the composition of the sample with maximum luminance being used for the training. There is no doubt that our case is not exceptional in this respect. Accordingly, the purpose of employing TANN in the present investigation was to refine the experimental data obtained from the conventional combinatorial chemistry process and to make them more succinct. Consequently, it can be concluded that TANN is not an appropriate method for global optimization but simply an auxiliary tool for understanding the screening results more completely.

Figure 4 shows the architecture of the artificial neural network (ANN) that was constructed for the QSAR modeling. This is a typical three-layered ANN consisting of input, hidden, and output layers. The input layer includes three units, each of which represents the molar fraction of SrO, B_2O_3, and P_2O_5, respectively. The hidden layer includes six units that are interlinked to the units on the input and output layers. The output layer involves only one unit, i.e., luminance. The CIE color coordinates x and y were omitted for convenience. This 3-6-1 architecture was determined by a huge number of optimization processes. Hyper tangent functions, along with biases, were adopted as transfer functions between the input and hidden layers, and linear bias functions were used between the hidden and output layers. The well-known back propagation method[21] was used for training. The data in the libraries for the first and the last fine-tuning given in Fig. 1b and c were adopted as a training set. As a result, a QSAR model was developed based on TANN. This implies that a continuous luminance map was obtained in place of the discrete combinatorial chemistry libraries in Fig. 1. The continuous map would be much more useful in both the design and optimization of new materials. A continuous luminance map obtained by our TANN is shown in Fig. 5. In this luminance map, an explicit line can be found on which high luminance and a single phase can be realized. This optimum line can be expressed by the following relation

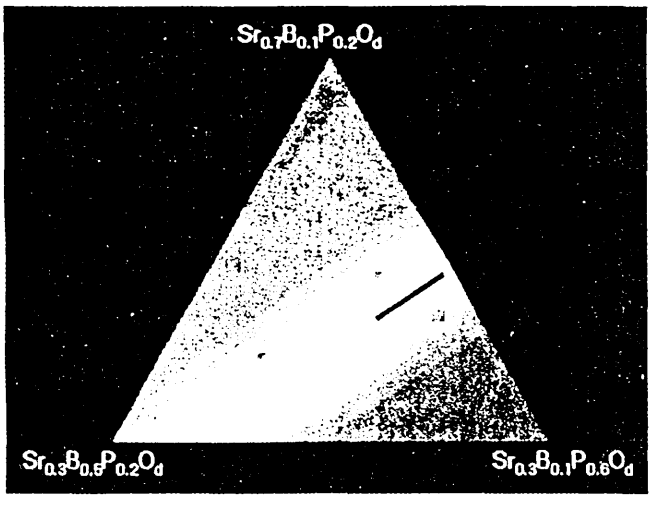

Figure 5. Continuous luminance map constructed by the trained artificial neural network.

$$Sr = 1.143\ P - 0.0048 \quad 0.77 < Sr + P < 0.9,\ 0.1 < B < 0.23 \qquad [1]$$

The compositions, which meet the requirements for the above relation, are not the exact stoichiometry of a resultant phase, indicating that if the initial composition setting satisfied the above relation, then a single-phase compound with a high luminance could be attained.

$Sr_6BP_5O_{20}:Eu^{2+}$ blue phosphor.— Six samples from the high-luminance region in the library for the final fine-tuning, i.e., samples a, b, c, d, 3, and 7 were analyzed by inductively coupled plasma–atomic emission spectrometry (ICP-AES) as well as the phase identification through structural analyses. The ICP-AES analysis showed that the Sr/P atomic ratio varied between 1.15 and 1.25 the Sr/B ratio was in the range from 4.12 to 5.75. Based on these results, the nearest chemical composition, using simple integers, suggests a composition of $Sr_6BP_5O_{20}$. On the basis of this estimate, the structure of the sample was examined by XRD measurements. Figure 6 shows a representative XRD pattern of sample 7. This pattern has never been reported in any previous studies, and thus, it cannot be found in any well-known databases including powder diffraction file II (PDFII) and inorganic crystallographic structure database (ICSD). The findings indicate that sample 7 consists of a major phase, in space group $I\bar{4}c2$, with cell parameters $a = 9.784$ and $c = 19.01$, together with a negligible amount (less than 1 vol %) of a minor phase $Sr_3(PO_4)_2$. The other five samples in the high-luminance region also contained this phase as the main phase. The samples outside the high-luminance region showed an enhanced portion of $Sr_3(PO_4)_2$ and $Sr_2P_2O_7$ phases, i.e., $Sr_3(PO_4)_2$ in the area above the high-luminance area and $Sr_2P_2O_7$ in the area beneath the high-luminance area.

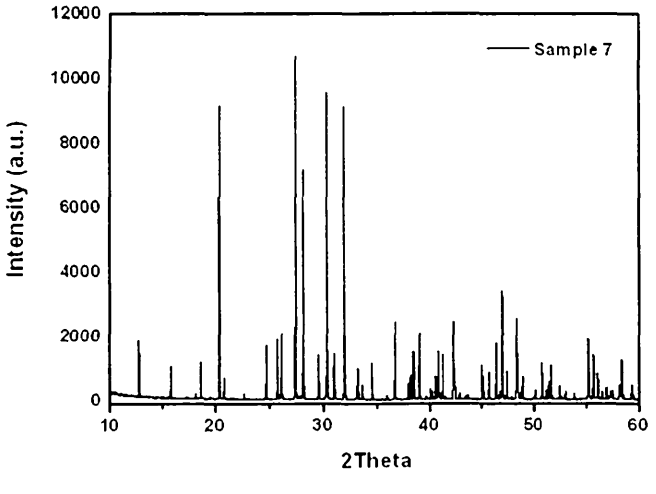

Figure 6. XRD patterns of sample 7.

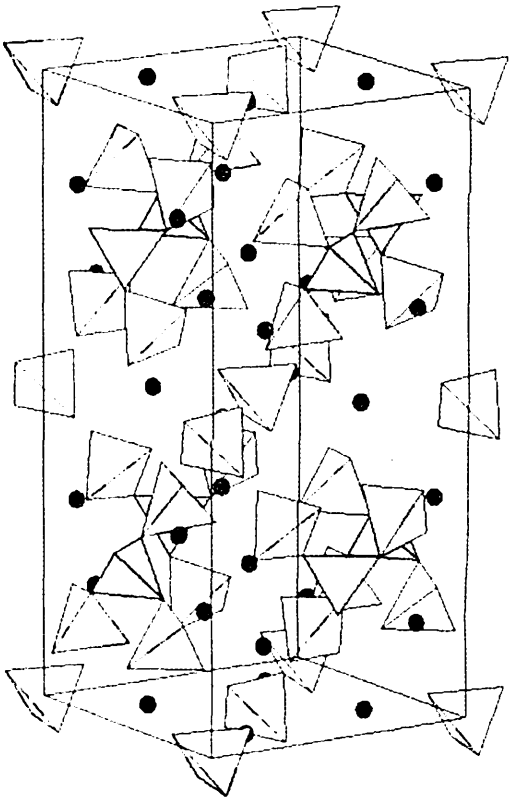

Figure 7. The exact structure of $Sr_6BP_5O_{20}$, as determined by ab initio calculation. The $[BO_4]$ tetrahedra were hatched in dark gray color and the $[PO_4]$ tetrahedra were not hatched. The sphere stands for Sr ions.

The major stoichiometric compound was determined to be $Sr_6BP_5O_{20}$, the exact structure of which has been recently clarified based on ab initio calculation by the authors.[23] This compound had been misled to be in the $P\bar{4}$ space group until we found the exact structure, because well-known similar compounds with the same stoichiometry such as $Pb_6BP_5O_{20}$[24] and $Pb_6BAs_5O_{20}$[25] are in the $P\bar{4}$ space group. However, the exact structure of $Sr_6BP_5O_{20}$ was proven to be in space group $I\bar{4}c2$, which is completely different from $Pb_6BP_5O_{20}$[24] and $Pb_6BAs_5O_{20}$[25] in the $P\bar{4}$ space group. Figure 7 shows the exact structure of $Sr_6BP_5O_{20}$ of $I\bar{4}c2$ symmetry, which exhibits a propeller-like structure consisting of the central $[BO_4]$ tetrahedron surrounded by the array of four $[PO_4]$ tetrahedral. Additional details of the structural analysis of $Sr_6BP_5O_{20}$ compound were presented in our recent report.[23]

The composition relation in Eq. 1 is slightly different from the $Sr_6BP_5O_{20}$ stoichiometry. When the initial composition was set at the exact $Sr_6BP_5O_{20}$ stoichiometry, the final product did not contain as much $Sr_6BP_5O_{20}$ phase as the composition setting obeying Eq. 1. As previously mentioned, the excessive amount of boron played a significant role in facilitating the reaction and, in turn, enhancing the luminance. Although the role of the excess boron cannot be clearly defined, we assumed that it could have a fluxing effect on the reaction. For further confirmation, we prepared several

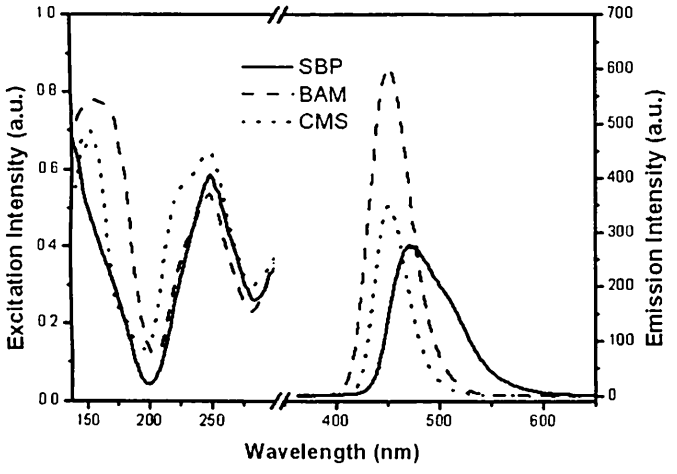

Figure 8. Excitation and emission spectra of SBP, CMS, and BAM.

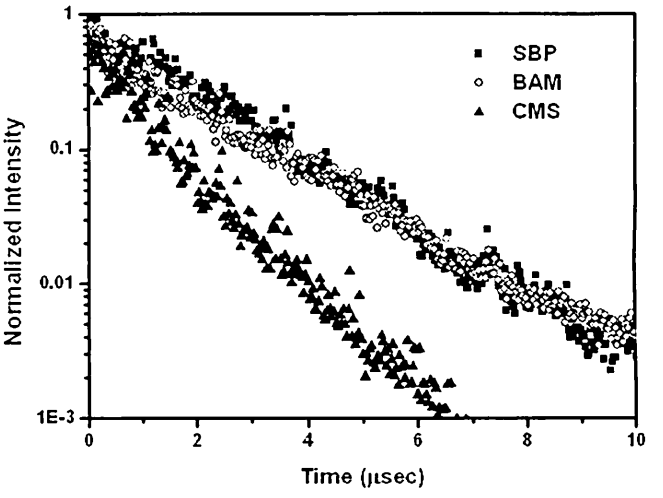

Figure 9. Decay curves of SBP, CMS, and BAM.

additional compounds, the starting compositions of which were $Sr_6B_xP_5O_{21.5}$ (x = 1–3 by a step of 0.2), and then compared them to the samples from the combinatorial libraries. It was found that luminance increased with x. The compounds with x values exceeding 2 were crystallized in the $Sr_6BP_5O_{20}$ phase with a negligible amount of minor phases and their luminance was comparable to sample 7.

The $Sr_6BP_5O_{20}$:Eu^{2+} blue phosphor, hereafter referred to as SBP, is not a new phosphor but had been developed in the 1970s for use in a high-color-rendering fluorescent lamp.[26] However, the luminescence of the SBP phosphor under VUV excitation has never been examined from the point of view of its use in PDP applications. In addition, the exact structure of the $Sr_6BP_5O_{20}$ stoichiometry had never been fully identified until we disclosed it. Accordingly, the systematic screening of the SrO–B_2O_3–P_2O_5 system enabled us to conclude that the SBP with a well-defined structure is a promising phosphor, suitable for PDP applications in view of its high luminescent efficiency under the VUV excitation.

The photoluminescent (PL) excitation and emission spectra of SBP were obtained under VUV excitation. The excitation and emission spectra are shown in Fig. 8, along with those for BAM and CMS phosphors, for comparison. We employed a commercially available BAM (Kasei), while the CMS was prepared by the conventional solid-state reaction method. It is obvious that all of the phosphors have a strong absorption at around 147 nm in the VUV region. The origin of the emission is the $4f^65d^1 \rightarrow 4f^7$ transition of Eu^{2+}, which shows a typical broad bandwidth. Even though the height of the emission spectrum of SBP appears to be lower than the others under conditions of VUV excitation as can be seen in Fig. 8, the luminance of SBP was estimated to be 280% that of BAM and 500% that of CMS by incorporating the standard visual spectral efficiency curve. It is obvious that the wavelength at the maximum of the emission spectrum of SBP (470 nm) is different from that of BAM and CMS (~420 nm), and, as a result, the CIE chromaticity coordinates are different (x = 0.144, y = 0.281 for SBP, and x = 0.145, y = 0.08 for BAM and CMS). This suggests that the color chromaticity of SBP is not as good as BAM and CMS at the current stage of development.

Time-resolved PL behavior was also monitored for these three blue phosphors. Figure 9 shows decay curves measured at an excitation of 355 nm with the emission probe at the emission peak wavelength of each phosphor. The 10% decay time of SBP, BAM, and CMS was estimated to be 3.5, 3.2, and 1.5 μs, respectively. The PL of CMS decayed more rapidly than SBP and BAM. Taking the straight line-shaped curves into account, it can be concluded that no significant nonradiative energy transfer occurred among Eu^{2+} ions for these Eu^{2+} contents. According to our auxiliary experiment, the concentration quenching began for a lot higher Eu^{2+} content, i.e., when the Eu^{2+} content reached 1/50 of Sr, the concentration quenching began to take place and, in turn, the decay curve of SBP became nonlinear.

It is more important to address the thermal stability of SBP compared to BAM. Figure 10 shows the thermal degradation behavior up to 700°C in terms of luminance for SBP, CMS, and BAM. These data show that the thermal stability of SBP and CMS is considerably superior to BAM in the temperature range from 500 to 700°C. In particular, SBP exhibited no thermal degradation at 500°C and only 5% even at 700°C. Considering the fact that the luminance of BAM decreased by more than 30% even at 500°C, SBP is clearly superior to BAM in terms of thermal stability. Unlike the BAM structure involving open layers on which Eu^{2+} ions can be located, SBP provides tight Eu^{2+} sites. Figure 10 also shows the local structures of Sr in SBP and Ba in BAM. Two possible Sr^{2+} (or Eu^{2+}) sites are enclosed by eight and nine oxygen ions with an average distance of 2.6729 and 2.7151 Å from the Eu^{2+} center, respectively.[24] The thermal degradation of BAM can be attributed to the loose local structure around the Ba^{2+} (or Eu^{2+}) site (nine oxygen ions in an average distance of 2.9512 Å from the Eu^{2+} center). Eu^{2+} ions can easily escape to other trivalent sites or open spaces by passing through the loosely associated oxygen ions in the case of BAM. Both of the

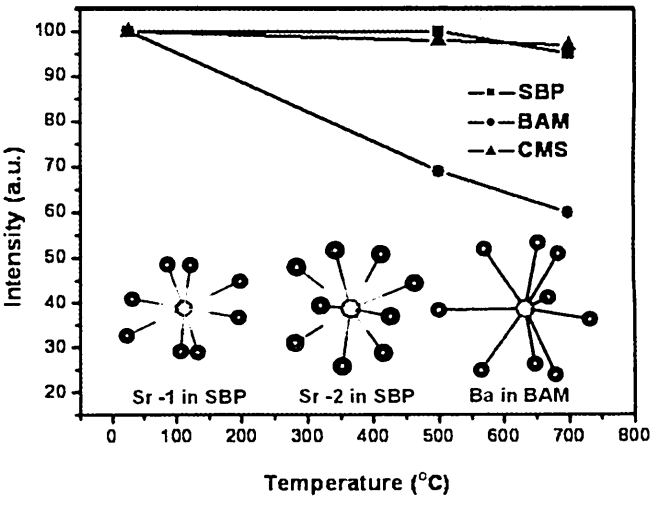

Figure 10. Thermal degradation in terms of luminance of SBP, CMS, and BAM. The inset shows the local structures of Sr in SBP and Ba in BAM.

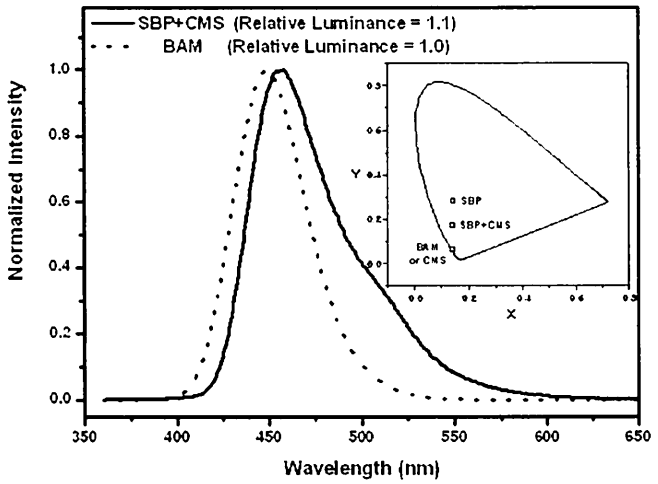

Figure 11. Normalized emission spectrum of the SBP–CMS mixture along with BAM. The inset shows the improvement in the CIE chromaticity coordinate y by the presence of CMS.

crystallographic sites for Sr^{2+} ions in SBP constitute a tight obstacle against the escape of Eu^{2+} ions. This could be the origin of the thermal stability of SBP.

Now that the luminescent efficiency and thermal stability of SBP have been examined, in compared to BAM and CMS, the next step is to discuss the color chromaticity of SBP. It is certain that color purity, which can be expressed as CIE chromaticity coordinates, is worse than that of BAM and CMS. A method for improving the color purity of SBP without losing thermal stability should be developed in order to effectively use SBP as a substitute for BAM in actual applications. Such a problem could be simply sorted out by employing another thermally stable blue phosphor such as CMS. CMS is also well known to be thermally stable.[8] A mixture of SBP and CMS showed improved CIE chromaticity coordinate values, but at the expense of luminance. Figure 11 shows the change in CIE chromaticity coordinates for a mixture of equal volume of CMS and SBP. Even though it cannot approach the standard blue color declared by the NTSC, the color chromaticity is closer to an acceptable level. In fact, the mixture of CMS to SBP has a CIE color chromaticity of $x = 0.145$, $y = 0.170$ and a luminance value 110% that of BAM. If it were possible to prepare an improved CMS, compared to that used in this experiment, both the luminance and color chromaticity of the mixture could be improved with the thermal stability maintained and the mixture could be a substitute for BAM. In addition, if SBP were mixed up with BAM, the SBP–BAM mixture could also be a tentative solution for mitigating the thermal degradation to a certain extent. Consequently, SBP could not be a complete, independent phosphor but a partial substitute for BAM, as far as PDP applications were concerned.

Conclusion

A Eu^{2+}-doped $SrO–B_2O_3–P_2O_5$ ternary system was screened through a three-step combinatorial chemistry process. Based on the results of the combinatorial screening, QSAR modeling was carried out by training an artificial neural network. As a result, a stochastic relationship between composition and luminance was obtained. Thus, it was possible to improve the discrete combinatorial library to give a continuous map-type library. The combinatorial chemistry and successive QSAR modeling process yielded SBP as an optimum phosphor, which is highly efficient under VUV excitation and is also thermally stable. The space group of the SBP was found to be $I\bar{4}c2$ with cell parameters $a = 9.784$ and $c = 19.01$. The exact structure of $Sr_6BP_5O_{20}:Eu^{2+}$ gave a plausible interpretation regarding the thermal stability in comparison to BAM.

The luminance was 280% higher than BAM, and thermal degradation at 700°C was 5%, at most. The CIE color chromaticity ($x = 0.145$, $y = 0.124$) was improved by blending SBP with a CMS phosphor, giving an acceptable luminance. The SBP-CMS mixed phosphor showed a CIE color chromaticity of $x = 0.145$, $y = 0.170$ and a luminance value 110% that of BAM with negligible thermal degradation. The acceptable luminance and the thermal stability of the SBP–CMS or SBP–BAM mixed phosphor would make it possible for use as a substitute for BAM phosphors, even though a slight deterioration in color chromaticity cannot be avoided.

Acknowledgment

This work was supported by grant no. R01-2002-000-00203-0 from the Basic Research Program of the Korea Science & Engineering Foundation. Experiments at PLS were supported in part by MOST and POSTECH.

Sunchon National University assisted in meeting the publication costs of this article.

References

1. N. Yocom, R. S. Meltzer, K. W. Jang, and M. Grimm, in *The 1st International Conference on the Science and Technology of Display Phosphors*, San Diego, CA, p. 27, (1995).
2. K.-S. Sohn, S. S. Kim, and H. D. Park, *Appl. Phys. Lett.*, **81**, 1759 (2002).
3. K.-B. Kim, Y.-I. Kim, H.-G. Chun, T.-Y. Cho, J.-S. Jung, and J.-G. Kang, *Chem. Mater.*, **14**, 5045 (2002).
4. K. C. Mishra, M. Raukas, A. Ellens, and K. H. Johnson, *J. Lumin.*, **96**, 95 (2002).
5. S. Oshio, K. Kitamura, T. Shigeta, S. Horii, T. Matsuoka, S. Tanaka, and H. J. Kobayashi, *J. Electrochem. Soc.*, **146**, 392 (1999).
6. S. Oshio, T. Matsuoka, S. Tanaka, and H. J. Kobayashi, *J. Electrochem. Soc.*, **145**, 3903 (1998).
7. S. Kubota and M. Shimada, *Appl. Phys. Lett.*, **81**, 2749 (2002).
8. T. Kunimoto, R. Yoshimatsu, K. Hhmi, S. Tanaka, and H. Kobayashi, *IEICE Trans. Electron.*, **E85-C**, 11 (2002).
9. J. Hao and M. Cocivera, *Appl. Phys. Lett.*, **79**, 740 (2001).
10. K.-S. Sohn, J. M. Lee, and N. Shin, *Adv. Mater. (Weinheim, Ger.)*, **15**, 2081 (2003).
11. K.-S. Sohn, I. W. Jeon, H. Chang, S. K. Lee, and H. D. Park, *Chem. Mater.*, **14**, 2140 (2002).
12. K.-S. Sohn, J. M. Lee, I. W. Jeon, and H. D. Park, *J. Electrochem. Soc.*, **150**, H182 (2003).
13. C. H. Kim, S. M. Park, J. G. Park, H. D. Park, K.-S. Sohn, and J. T. Park, *J. Electrochem. Soc.*, **149**, H21 (2002).
14. S. Y. Seo, K.-S. Sohn, H. D. Park, and S. J. Lee, *J. Electrochem. Soc.*, **149**, H12 (2002).
15. S. Shionoya and W. M. Yen, *Phosphor Handbook*, p. 623, CRC Press, Boca Raton, FL (1999).
16. M. V. Hoffman, *J. Electrochem. Soc.*, **115**, 560 (1968).
17. T. Hattori and S. Kito, *Catal. Today*, **23**, 347 (1995).
18. M. Sasaki, H. Hamada, Y. Kintaichi, and T. Ito, *Appl. Catal., A*, **132**, 261 (1995).
19. Z.-Y. Hou, Q. Dai, X.-Q. Wu, and G.-T. Chen, *Appl. Catal., A*, **161**, 183 (1997).
20. Y. Watanabe, T. Umegaki, M. Hashimoto, K. Omata, and M. Yamada, *Catal. Today*, **89**, 455 (2004).
21. U. Rodemerck, M. Baerns, M. Holena, and D. Wolf, *Appl. Surf. Sci.*, **223**, 168 (2004).
22. J. C. Principe, N. R. Euliano, and W. C. Lefebvre, *Neural and Adaptive System*, John Wiley & Sons, Inc., New York (2000).
23. N. Shin, J. Kim, D. Ahn, and K.-S. Sohn, *Acta Crystallogr., Sect. C: Cryst. Struct. Commun.*, **61**, i54 (2005).
24. R. Kniep, H. Engelhardt, and C. Hauf, *Chem. Mater.*, **14**, 2930 (1998).
25. E. L. Belokoneva, E. A. Ruchkina, O. V. Dimitrova, and S. Y. J. Stefanovuch, *Inorg. Chem.*, **46**, 179 (2001).
26. K. Murakami, Y. Anzai, H. Itoh, S. Doi, and K. Awazu, *Technical Digest of the Phosphor Research Society, 173rd Meeting*, p. 701 (1978).